Accepted by ASCE Journal of Materials in Civil Engineering, 2011.

Using Viscosity Modifiers to Reduce Effective Diffusivity in Mortars

Kenneth A. Snyder
Dale P. Bentz
Engineering Laboratory

Jeffrey M. Davis
Material Measurement Laboratory
National Institute of Standards and Technology
Gaithersburg, MD 20899

Abstract

Three viscosity modifiers (a commercial shrinkage-reducing admixture, a polypropylene glycol, and cellulose ether) are used to reduce the effective diffusivity of chloride ions through mortars during a one-year exposure. Two delivery mechanisms were studied: adding a viscosity modifier to the mix water; and diluting the viscosity modifier in water, pre-wetting fine lightweight aggregate (LWA) with the solution, and replacing a portion of the sand with the pre-wetted LWA, which is equivalent to the practice of using LWA for internal curing. After a 28-day curing period, the cylinders were submerged in a 1 mol/L chloride solution. After 24 weeks and 52 weeks of exposure, micro X-ray fluorescence analysis was used to profile the radial chloride concentration under ambient air pressure. The effective diffusivity was estimated by regression, assuming ideal Fickian radial diffusion. Compared with the control mortar (no admixture, no LWA), the addition of the viscosity modifier to the mix water reduced the effective diffusivity by nearly a factor of two, and using LWA saturated with a viscosity modifier reduced the effective diffusivity by a factor greater than two. Therefore, the use of these viscosity modifiers has the potential to double the service life of any concrete that may be subjected to degradation that depends upon diffusion, such as corrosion of the steel reinforcement and sulfate attack.

Keywords: Diffusion; lightweight aggregate; micro X-ray fluorescence; mortar; service life; viscosifier; viscosity.

Introduction

In the 21st century, sustainability has emerged as a key concern of the construction community and society at large [1]. A major contributor to the sustainability of a concrete structure is its service life because, when considered over a very long time, the environmental and economic impacts are in proportion to the number of times the structure has to be repaired or replaced. In many degradation scenarios, including chloride-induced corrosion of steel reinforcement and external sulfate attack, the rate of diffusion of a deleterious species from the environment into the concrete largely controls its service life [2]. Conventionally, one reduces the effective diffusivity of these species in concrete by reducing the porosity and increasing the

tortuosity of the hydrated cement paste through strategies such as reducing the water-to-cementitious materials ratio (*w/cm*) and/or adding supplementary cementitious materials. These approaches, however, may also increase the likelihood of early-age cracking, with these cracks providing preferential pathways for ion ingress [3].

With this in mind, an alternate paradigm for decreasing effective diffusivity has been developed through the introduction of appropriate viscosity modifiers into the concrete pore solution [4-6]. These viscosifiers may be added directly to the mix water, in a manner equivalent to that employed for most conventional chemical admixtures, or a diluted solution of the viscosifier may be used to pre-wet fine lightweight aggregates. For the latter case, as the cement hydrates, this solution will be drawn out of the lightweight aggregates into the surrounding cement paste due to the chemical shrinkage and self-desiccation that accompanies cement hydration [7].

As this viscous solution is drawn from the LWA into the pore solution, the viscosity of the pore solution will increase. According to the Stokes-Einstein relation, the self-diffusion coefficient of an ion is inversely proportional to the viscosity (or hydrodynamic friction) of the solution in which it is diffusing; thus, doubling the viscosity of the pore solution should reduce the effective diffusivity by a factor of two [8], in turn doubling the service life of the concrete in many degradation scenarios. This new technology for doubling concrete service life has been given the acronym VERDiCT: Viscosity Enhancers Reducing Diffusion in Concrete Technology.

The objectives of the present study are to extend the preliminary evaluations of the VERDiCT technology in mortars [6], by considering two water-to-cement mass ratios (*w/c*=0.4 and 0.45) and three viscosifiers, and to obtain a more detailed quantitative analysis of the chloride ion profiles based on micro X-ray fluorescence. The latter allows a quantitative estimate of effective diffusivities to be obtained, including their uncertainties. In addition, thermogravimetric analysis (TGA) is used to examine the fate of the viscosifiers within the hydrated cement paste microstructure.

Materials and Experimental Procedures

An ASTM C150 Type II/V [9] low alkali cement (that also qualifies as a Type I) was employed in all mortar mixtures. It had a Blaine fineness of 387 m^2/kg, a density of 3220 kg/m^3, and an ASTM C150 computed Bogue composition of 61 % tricalcium silicate, 15 % dicalcium silicate, 5 % tricalcium aluminate, and 13 % tetracalcium aluminoferrite by mass, with a sodium oxide equivalent of 0.31 %. A mixture of four silica sands, each with a density of 2610 kg/m^3, was used in each mortar. The fine lightweight aggregate was a commercial expanded shale with a saturated surface dry (SSD) water absorption of 22 % by mass at 25 ^oC, and a measured water desorption of approximately 20 % by mass at 25 ^oC when the SSD aggregates were exposed to a humid environment in equilibrium with a slurry of potassium nitrate (relative humidity of 93 %). The measured SSD density was (1800 ± 50) kg/m^3 (one standard deviation). For all mixtures, the total sand (normal + LWA) volume fraction was kept constant at 0.55, and the LWA was substituted for a similar size distribution of normal weight sand on a volume basis.

Three viscosity modifiers were identified as having the potential to reduce the diffusivity of chloride ions: a polyoxyalkylene alkyl ether commercially available shrinkage-reducing admixture (denoted by the letter T), a polypropylene glycol with a molar mass of approximately 400 g/mol (P), and a high molecular mass (> 10,000 g/mol) cellulose ether viscosifier (C). The expected effectiveness of each admixture was ascertained from solution conductivity measurements. The relative effect that an admixture (and its concentration) has on reducing the chloride diffusivity should be in proportion to the relative effect the admixture has on the reducing the relative conductivity of potassium chloride solution. The details of this measurement process were described previously [4]. For this study, viscosifiers T and P were employed at a content equivalent to 10 % (by mass) of the mix solution (mix water + viscosifier), while C was used at a content equivalent to only 0.3 % (by mass), as it is a much more effective viscosifier. At these concentrations, each viscosifier produced a solution with a viscosity approximately double that of water, and viscosifiers T and P significantly reduced the measured electrical conductivity of this solution, while viscosifier C increased it slightly.

Mortars were prepared at *w/c* of 0.40 and 0.45, with their mixture designs being provided in Table 1 and Table 2, respectively. In these tables, the sample name indicates the *w/c*, type of viscosifier used, and the delivery mechanism. The first two numbers indicate the *w/c*. The first letter for each mixture designates the composition of the mix water: W=distilled water (control), T=polyoxyalkylene alkyl ether in water, P=polypropylene glycol in water, and C=cellulose ether in water. The 2nd letter indicates the presence or absence of LWA in the mixture: x=absent, and L=LWA is present. The 3rd letter indicates the chemical solution used to pre-wet the LWA when it is present: x= LWA absent, (W, T, or P) = LWA is saturated with the aforementioned viscosifier solution.

Table 1 and Table 2 also include the estimated air content, as calculated by ASTM C185 [10] at the time of mixing. The majority of these air content values range from 2 % to 4 %. The air content is greatest in the cellulose ether mixes, which suggests that this admixture may be acting as an air-entraining agent.

Table 1. Mixture designs for the mortar mixtures with *w/c*=0.4. Air content is calculated using ASTM C185 [10] at the time of mixing.

	Wxx	**Txx**	**Pxx**	**Cxx**	**WLW**	**WLT**	**WLP**
Cement (g)	3125	3125	3125	3125	3125	3125	3125
Mix water (g)	1250	1184	1184	1250	1250	1250	1250
Sand (g)	7006	7209	7209	7006	5247	5247	5247
Viscosifier in mix water (g)	0	132	132	4	0	0	0
LWA (g)	0	0	0	0	994	994	994
Water in LWA (g)	0	0	0	0	219	80	80
Viscosifier in LWA (g)	0	0	0	0	0	139	139
Air Content (%)	1.42	2.16	2.93	4.84	3.46	3.85	3.70

Table 2. Mixture designs for the mortar mixtures with *w/c*=0.45. Air content is calculated using ASTM C185 [10] at the time of mixing.

	Wxx	**Txx**	**Pxx**	**Cxx**	**WLW**	**WLT**	**WLP**
Cement (g)	3000	3000	3000	3000	3000	3000	3000
Mix water (g)	1350	1279	1279	1350	1350	1350	1350
Sand (g)	7182	7095	7095	7182	5206	5206	5206
Viscosifier in mix water (g)	0	142	142	4	0	0	0
LWA (g)	0	0	0	0	954	954	954
Water in LWA (g)	0	0	0	0	210	60	60
Viscosifier in LWA (g)	0	0	0	0	0	150	150
Air Content (%)	1.92	0.44	2.07	6.03	2.17	3.68	4.16

Mortars were prepared in a planetary mixer using the mixing procedures outlined in ASTM C305 [11]. For each mortar mixture, twelve 50 mm x 100 mm mortar cylinders were cast and cured in sealed bags for 24 h. Mortars not containing LWA were demolded after 24 h and placed in a curing solution until an age of 28 d. This curing solution was prepared as a mixture of potassium, sodium, and calcium hydroxides. The concentration of hydroxides in each curing solution is given in Table 3, and the values were chosen to approximately match the alkali composition of the mortar specimens' internal pore solution. Mortars containing LWA were cured under sealed conditions by double wrapping them in two sealed plastic bags until an age of 28 d. Sealed curing was selected for these mixtures to promote the migration of the viscosifier/water solution from within the LWA into the surrounding hydrating cement paste [6], and to mimic the conditions expected in the field.

Table 3. Concentration (mol/L) of hydroxides in the curing solutions used for mortars without LWA.

	mol/L	
Hydroxide	***w/c* = 0.40**	***w/c* = 0.45**
KOH	0.0948	0.0843
NaOH	0.0178	0.0158
$Ca(OH)_2$	0.0034	0.0040

At the end of each curing period, the mortar cylinders were each submerged in 600 mL of a 1 mol/L sodium chloride solution that was contained in a sealable plastic bottle. After exposure times of 24 weeks and 52 weeks, sample cylinders were removed from their jars and evaluated for chloride penetration. At the designated exposure age, two cylinders were removed from their solution and split lengthwise using a universal testing machine. For each cylinder, one exposed surface was analyzed using micro X-ray fluorescence (μXRF); the relatively high NaCl concentration was chosen to ensure that there would be sufficient μXRF signal. Small fragments of some of the mortars were subjected to TGA analysis, by heating to a temperature of 1000 °C at a heating rate of 10 °C/min.

Isothermal Calorimetry

A subset of the mortars was also evaluated for the influence of the viscosifiers on cement hydration rates using isothermal calorimetry. For each mortar mixture, two glass vials were loaded with approximately 8 g of fresh mortar and placed in the calorimeter, along with a reference vial containing dry cement powder. Heat release was then monitored out to an age of 7 d. The results in Figure 1 generally indicate a mild retardation due to the presence of a viscosifier, with the exception of the cellulose ether that produced curves quite similar to those of the control (no viscosifier) mixture. Introducing the viscosifier via the LWA, as opposed to via direct addition to the mixing water, reduced the effect of the retardation and increased the achieved hydration (particularly in the longer term for the *w/c* =0.4 mortars). This increase in longer term hydration has been noted previously for mortar mixtures with internal curing using LWA pre-wetted with only water [6, 12].

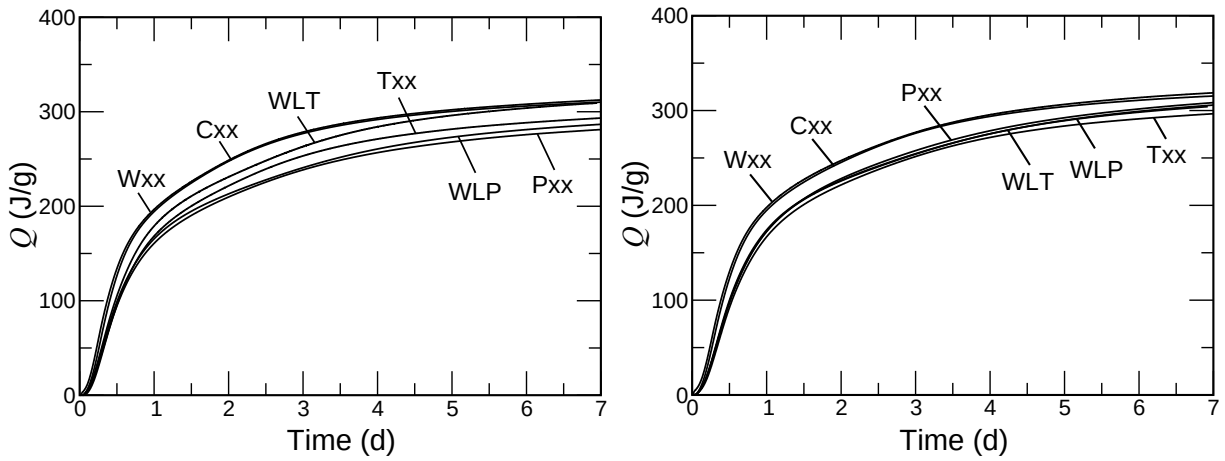

Figure 1. Cumulative heat release *Q*, per gram of cement, up to 7 d hydration for mortar mixtures with *w/c*=0.4 (left) and *w/c*=0.45 (right).

Micro X-ray Fluorescence

Micro X-ray fluorescence (μXRF) has been used elsewhere to effectively track infiltrating ions in concrete [13]. By exciting a polychromatic X-ray beam using a rhodium target, the major and minor constituents of the cement paste and aggregate can be easily identified. Further, by focusing the beam using a polycapillary optic, the beam spot can be manipulated to excite an area only 80 μm in diameter. The principle advantage to μXRF over other X-ray microanalytical techniques (such as SEM-EPMA [14]) is the ability to extract elemental images from a heterogeneous surface, at atmospheric pressure and without the same surface smoothness requirements as many other techniques.

Early experiments designed to optimize the measurement protocol revealed that certain considerations were necessary to ensure accurate, reliable measurements. First, applying a vacuum to the system, which improves the detection sensitivity to light elements, tends to dry out the concrete specimen and force chloride ions further into the specimen. Since μXRF is a surface technique, a removal of ions from the surface will severely impact the results. Second, since the system uses polychromatic rhodium (Rh) radiation, the Rh Lα X-ray line will overlap with the chlorine (Cl) Kα X-ray line, significantly increasing the lower limit of detection for Cl and making the background very difficult to model. A 25 μm thick Al foil was used to prevent the Rh Lα radiation from reaching the sample, thereby eliminating the Rayleigh scatter Rh peak from the spectrum. The effective background in the Cl region is very low with the Al foil in place. Finally, although μXRF is not as sensitive to surface roughness as electron microscope based techniques, some consideration is required to produce high quality images and spectra. Random roughness induced by breaking the cylinder was on the order of 0.5 mm over a field of view, although global variations in the surface could be several millimeters. Careful visual inspection of the surface was necessary to mark out an area with no major variations for analysis. Each field of view was sufficiently large to include a large number of aggregates, thus ensuring a representative sample.

Given the considerations mentioned, the optimal measurement protocol was as follows. The samples were imaged using a point-to-point distance of 80 μm in both the *z* (longitudinal) and *r* (radial) directions, with typically 200 points in the *z* direction and 300 points in the *r* direction. At each measurement point, a full X-ray spectrum up to 10 keV was acquired for 1 s, using a Si(Li) energy dispersive spectrometer (EDS), with a resolution of 165 eV at 5.9 keV. The X-ray data were stored in a binary database, which was later interrogated with NIST developed Lispix software [15]. Each measurement took approximately 18 h, and was typically run overnight. Samples were measured at atmospheric pressure and ambient temperature for all experiments.

Effective Diffusivity

The effective chloride diffusivity for each cylinder was estimated by assuming ideal radial Fickian diffusion in a cylindrical coordinate system. The concentration $C(r,t)$ at radial position *r* and time *t* for a cylinder having radius *R*, an initial internal background concentration C_b, and in contact with a constant concentration C_s at the surface,[1] can be expressed analytically [16, Eq. 5.22]:

$$\frac{C(r,t)-C_b}{C_s-C_b}=1-\frac{2}{R}\sum_{n=1}^{\infty}\frac{\exp\left(-\alpha_n^2 Dt\right)\ J_o(\alpha_n r)}{\alpha_n J_1(\alpha_n r)} \tag{1}$$

The parameter *D* is the Fickian diffusivity of the species of interest. The quantities J_o and J_1 are the Bessel functions of first kind having order zero and one, respectively [17]. Each value of a_n satisfies the positive roots of the following equation:

$$J_o(a_n R)=0 \tag{2}$$

Here, it is assumed that the μXRF chloride count is proportional to the concentration of chloride ions. Therefore, the μXRF counts are surrogates for concentration, and Eq. 1 has three unknown parameters: the Fickian diffusivity *D*, the background counts C_b, and the surface counts C_s. Even though there are only three adjustable parameters and hundreds of measurements, the estimated result for *D* at early ages can depend strongly on the estimated background value.

Fortunately, there is an independent means of estimating the background value. Before each measurement, the X-ray flux was adjusted to a constant value using a standard target. Given that the aggregate fraction was kept constant, and that the cement paste microstructures were similar for all specimens, it would be a reasonable estimate to assume that the chloride background count for all specimens at the same age of chloride exposure would be approximately constant. From a spectral analysis of the detected X-rays, one can determine the fraction of counts to be attributed to the chloride peak, and the remaining fraction that should be attributed to the background. Although this doesn't indicate *which* counts are due to chlorides

[1] It is being assumed that the external concentration of chloride is constant, as the 600 mL of available solution provides a large (nearly constant) reservoir of chloride ions.

and *which* are due to the background, it is an indication of the number fraction that should be attributed to the background.

Assuming that these background counts are randomly distributed uniformly across the entire image, one could estimate the average background value that should be attributed to each pixel in the image, thus yielding the background value C_b. Taking the values from all the specimens at a given age provided a means of estimating the uncertainty (expressed as the estimated standard deviation). At 24 weeks the estimated average background was (8.22 ± 0.29), and at 52 weeks this value was (9.03 ± 0.31); the reported uncertainty is the standard deviation of the population, and indicates the relatively constant values observed throughout the study.

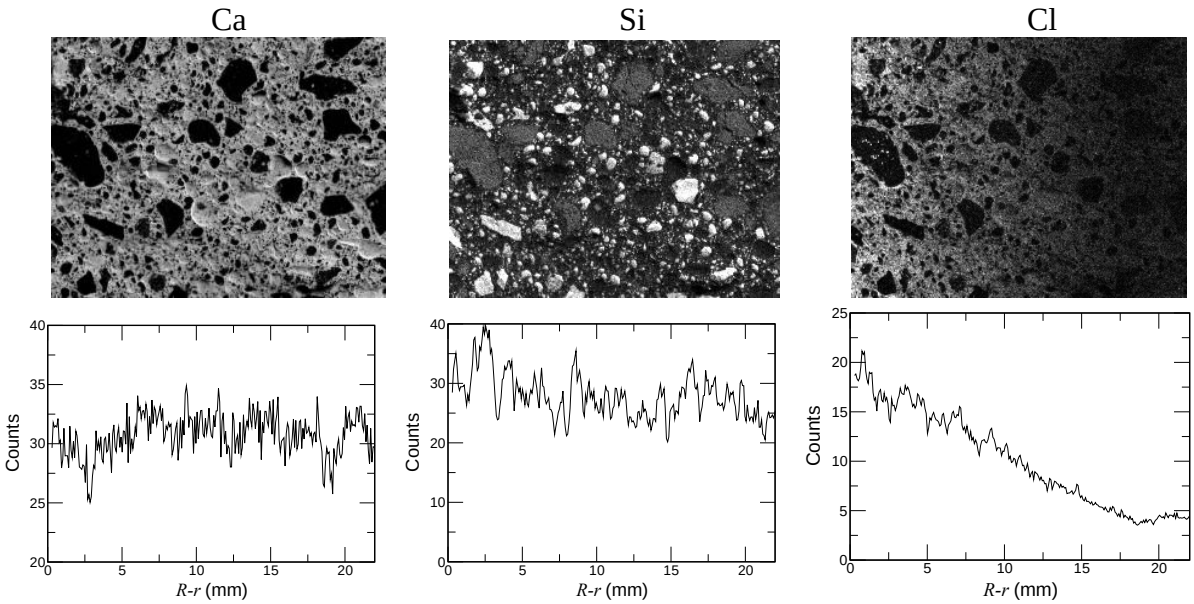

Figure 2. Image maps (22.0 mm wide, 17.0 mm high) for calcium (left), silicon (middle), and chlorine (right) for sample 40WLT-3 after 24 weeks of exposure. The sample surface is 250 μm beyond the left side of each image. Below each image is a plot of the average intensity for each column of pixels.

The outputs from the μXRF measurements were 2-dimensional images of the sample, with the intensity representing the signal strength for a particular element. Figure 2 shows typical element images (mortar 40WLT after 24 weeks of chloride exposure) for calcium (Ca), silicon (Si), and chlorine (Cl), along with a graph showing the average number of counts in each column. The data begin 250 μm from the outside surface because there is signal fall-off at the edge of the sample. The chlorine profile indicates that the background value is below the value of 8.22 from the spectral analysis. Upon a closer comparison among the elemental maps, one can see that neither the (silica-rich) sand nor the LWA (medium grey in the Si map) contribute to the chloride map. Therefore, the spectral analysis considers only those pixels that contribute counts to the chloride map, which does not include either aggregate. This means that the estimated chloride background is the paste fraction (0.45) times the previous background values: 3.70 at 24 weeks, and 4.06 at 52 weeks. Because this approach is still an approximation, the uncertainty attributed to both these values is 1.0, representing one standard deviation.

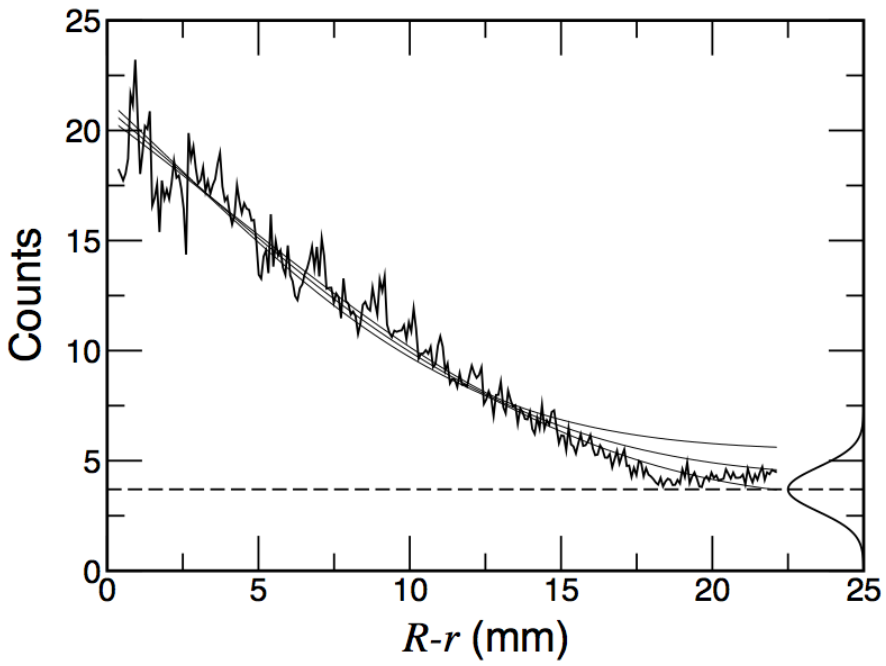

Figure 3. The scaled chloride profile, expressed as a function of the radial distance r, in a cylinder having radius R. The horizontal dashed line is the calculated background value C_b, and the Gaussian curve shows the uncertainty associated with the background value. The middle of the three curves represents the average profile, and the bounding curves represent the 95th percentiles for the predicted profiles.

An estimate for the uncertainty in the background value provided a means of estimating the uncertainty in the diffusivity D. For a fixed background value C_b, one can perform a two-parameter regression to find best estimates for D and C_o. Because uncertainty in the estimated background is quantified, a population of D values is obtained by sampling over the distribution for C_b. Figure 3 depicts the outcome of the analysis performed for the sample shown in Figure 2. The horizontal dashed line denotes the estimated background value of 3.70, and the Gaussian curve denotes the uncertainty (standard deviation equals 1) in this value. Repeatedly performing the regression, using samples from the Gaussian for the background, yields a distribution of diffusivities (D), surface concentrations (C_o), and profiles. The three smooth curves in Figure 3 represent the population of profiles: the middle curve is the average, and the upper and lower curves represent the 95-th percentiles of the population of curves recorded at that value of R-r.

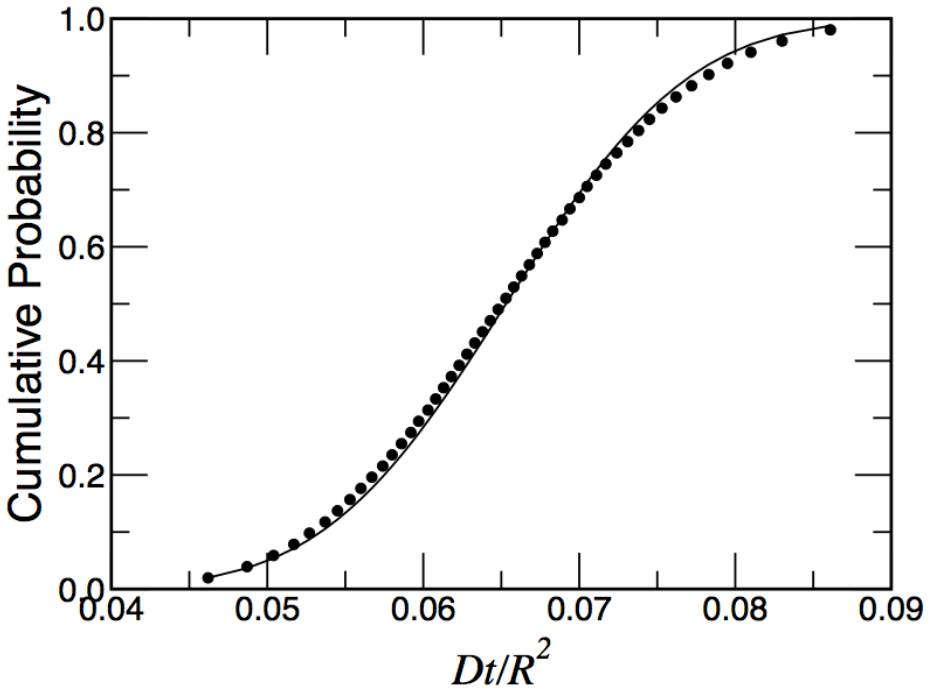

Figure 4. The measured and estimated probability function for the values of Dt/R^2 calculated for 40WLT-3. The filled circles are the calculated values for different C_b values, and the curve is the probability function of a normal distribution having the same mean and standard deviation.

To make a quantitative statement about the expanded uncertainty [18] in the reported value of Dt/R^2, one needs to ascertain the probability distribution function of the population of values. Because the values of C_b were normally distributed, the assumption was that the values of Dt/R^2 would also be normally distributed. The calculated values of Dt/R^2 from the regression results in Figure 3 are shown as filled circles in Figure 4. The x-value is the calculated parameter from the regression, and the y-value is the cumulative probability of the corresponding measured values. The mean and standard deviation of the values were (0.0653 ± 0.0092). The smooth curve in the figure is the normal probability function for a distribution with the same mean and standard deviation. As can be seen in the figure, the population of Dt/R^2 values is approximated reasonably well by a normal distribution. Therefore, the coverage factor of the reported standard deviations is roughly equivalent to that for one standard deviation of a normal distribution.

Results and Discussion

At the prescribed time of exposure, two cylinders were removed from their container, towel dried, split in two longitudinally, and sealed in a jar until the measurement was made (within four days of splitting); one chloride profile was made from each of the two cylinders. In some cases, either instrumentation or scheduling problems allowed for only a single chloride profile.

Mass Change

The mass of each cylinder (saturated, surface dry) was determined prior to exposure to chloride solution, and then again just before splitting. The mass increase between the time of exposure and the time of testing is given in Table 4 below, where the change is expressed as a percentage. The data indicate that the cylinders continued to absorb liquid between 24 weeks and 52 weeks of exposure. There are two noteworthy facts from these data: the presence of VERDiCT and LWA appear to have a greater influence on the mass change than the *w/c* binder ratio; and the minor mass increase for the cellulose ether (Cxx) mixes, which had the greatest air contents, suggests that the air voids in these systems are no more saturated than the Wxx specimens.

Table 4. Cylinder mass increase (expressed as a percent) that occurred between the beginning of chloride exposure and the time of testing. Two values were determined for each mixture, at each exposure time.

	Mass Increase (%)	
Mixture	**24 weeks**	**52 weeks**
40Wxx	0.17, 0.21	0.30, 0.30
40Txx	0.52, 0.46	0.69, 0.78
40Pxx	0.59, 0.64	0.84, 0.85
40Cxx	0.21, 0.26	0.39, 0.34
40WLW	0.51, 0.55	0.69, 0.74
40WLT	1.18, 1.22	1.55, 1.55
40WLP	1.59, 1.69	2.26, 2.30
45Wxx	0.21, 0.13	0.30, 0.30
45Txx	0.47, 0.47	0.61, 0.63
45Pxx	0.60, 0.64	0.77, 0.68
45Cxx	0.26, 0.27	0.40, 0.40
45WLW	0.78, 0.82	1.01, 0.94
45WLT	1.41, 1.47	1.71, 1.79
45WLP	1.95, 2.01	2.65, 2.34

Surface Concentration

The variability of the estimated surface concentration C_s is an indication of the uniformity among the samples and the measurement process. The estimated C_s values are given in Table 5.

Although the values increase slightly from 24 weeks exposure to 52 weeks exposure, the values are relatively constant among samples of the same exposure, regardless of *w/c* value. For the two instances of no reported values, the penetration was so significant that a determination of C_s was not possible.

Table 5. Mean values of surface concentration C_s (chloride counts) for both the *w/c* = 0.40 and the *w/c* = 0.45 samples. The reported uncertainty is the population standard deviation of the C_s values from the Monte Carlo calculation. In some cases, only one measurement was possible. For the two cases of unreported values, the chloride ingress was so severe that an estimate was not possible.

	Cs	
Mixture	**24 weeks**	**52 weeks**
40Wxx	(34.68 ± 0.05)	(39.06 ± 0.01) (42.49 ± 0.00)
40Txx	(36.52 ± 0.19)	(46.60 ± 0.04) (37.55 ± 0.01)
40Pxx	(33.40 ± 0.16) (35.13 ± 0.11)	(41.37 ± 0.01)
40Cxx	(22.40 ± 0.06) (32.40 ± 0.05)	(42.26 ± 0.00) (38.54 ± 0.00)
40WLW	(29.88 ± 0.09)	(42.22 ± 0.01)
40WLT	(20.99 ± 0.20) (25.62 ± 0.27)	(39.02 ± 0.04) (47.61 ± 0.07)
40WLP	(31.15 ± 0.17) (39.08 ± 0.12)	(45.63 ± 0.02)
45Wxx	(33.63 ± 0.00) (33.58 ± 0.03)	(41.30 ± 0.00) (43.81 ± 0.00)
45Txx	(35.06 ± 0.11) (34.48 ± 0.07)	(40.50 ± 0.00) (41.94 ± 0.01)
45Pxx	(23.73 ± 0.02) (36.36 ± 0.03)	(41.30 ± 0.00) (38.33 ± 0.00)
45Cxx	(29.34 ± 0.00) (30.68 ± 0.00)	
45WLW	(35.89 ± 0.02)	(40.27 ± 0.00)
45WLT	(27.01 ± 0.08) (28.74 ± 0.21)	(42.15 ± 0.03)
45WLP	(26.74 ± 0.06) (32.35 ± 0.13)	

Fickian Diffusivity

The Fickian diffusion coefficient is the primary material parameter that, along with the sample geometry, determines the time span before the onset of degradation. As these mortars do not represent concrete, the specific values of diffusivity are not important. Instead, the dimensionless quantity Dt/R^2 is convenient because it yields a number having a magnitude near one, and can be converted to diffusivity using the cylinder radius *R and the exposure time t*.

The estimated values of the dimensionless parameter Dt/R^2 for each observed cylinder are given in Table 6. The values in parentheses denote the average and standard deviation of the Dt/R^2 values, as calculated from the regression calculations. For the two instances of no reported values, the penetration was so significant that a determination of Dt/R^2 was not possible.

Table 6. Estimated values of the dimensionless parameter Dt/R^2 from each observed cylinder. The reported uncertainty is the population standard deviation of the Dt/R^2 values from the Monte Carlo calculation. In some cases, only one sample was analyzed. For the two cases of unreported values, the chloride ingress was so severe that an estimate was not possible.

	Dt/R^2	
Mixture	**24 weeks**	**52 weeks**
40Wxx	(0.1130 ± 0.0054)	(0.1979 ± 0.0047) (0.2840 ± 0.0042)
40Txx	(0.0819 ± 0.0055)	(0.1348 ± 0.0040) (0.1880 ± 0.0050)
40Pxx	(0.0856 ± 0.0061) (0.0888 ± 0.0054)	(0.1881 ± 0.0044)
40Cxx	(0.0994 ± 0.0088) (0.1060 ± 0.0058)	(0.2044 ± 0.0043) (0.2501 ± 0.0047)
40WLW	(0.1023 ± 0.0067)	(0.1951 ± 0.0043)
40WLT	(0.0653 ± 0.0092) (0.0623 ± 0.0077)	(0.1335 ± 0.0049) (0.1290 ± 0.0041)
40WLP	(0.0847 ± 0.0065) (0.0912 ± 0.0049)	(0.1689 ± 0.0040)
45Wxx	(0.1955 ± 0.0054) (0.1503 ± 0.0056)	(0.4077 ± 0.0043) (0.3620 ± 0.0041)
45Txx	(0.1109 ± 0.0058) (0.1199 ± 0.0057)	(0.2659 ± 0.0045) (0.2243 ± 0.0043)
45Pxx	(0.1568 ± 0.0084) (0.1331 ± 0.0051)	(0.2541 ± 0.0044) (0.2412 ± 0.0048)
45Cxx	(0.2213 ± 0.0064) (0.2090 ± 0.0060)	
45WLW	(0.1723 ± 0.0052)	(0.5244 ± 0.0045)
45WLT	(0.1111 ± 0.0076) (0.0871 ± 0.0076)	(0.1607 ± 0.0045)
45WLP	(0.1154 ± 0.0075) (0.0965 ± 0.0062)	

For the entries in Table 6 that consist of two measurements, a single expression for Dt/R^2 can be obtained by calculating the average and propagating the errors. The resulting values are given in Table 7. This condensed representation facilitates a direct comparison between pairs of specimens. Note how the values of Dt/R^2 roughly double, as they ought, from 24 weeks to 52 weeks. This suggests that the chlorides are being transported primarily by Fickian diffusion; there is relatively little binding, absorption, or reaction occurring during this time period. The notable exception to this is the w/c=0.45 WLW specimens, which is discussed later.

Table 7. The estimated values of Dt/R^2 below are the average of the values in Table 6, and the uncertainty (one standard deviation) represents the propagation of errors.

	Dt/R^2	
Mixture	**24 weeks**	**52 weeks**
40Wxx	(0.1130 ± 0.0054)	(0.2410 ± 0.0032)
40Txx	(0.0819 ± 0.0055)	(0.1614 ± 0.0032)
40Pxx	(0.0872 ± 0.0041)	(0.1881 ± 0.0044)
40Cxx	(0.1027 ± 0.0053)	(0.2273 ± 0.0032)
40WLW	(0.1023 ± 0.0067)	(0.1951 ± 0.0043)
40WLT	(0.0638 ± 0.0060)	(0.1313 ± 0.0032)
40WLP	(0.0880 ± 0.0041)	(0.1689 ± 0.0040)
45Wxx	(0.1729 ± 0.0039)	(0.3849 ± 0.0030)
45Txx	(0.1154 ± 0.0041)	(0.2451 ± 0.0031)
45Pxx	(0.1450 ± 0.0049)	(0.2477 ± 0.0033)
45Cxx	(0.2090 ± 0.0044)	
45WLW	(0.1723 ± 0.0052)	(0.5244 ± 0.0045)
45WLT	(0.0991 ± 0.0054)	(0.1607 ± 0.0045)
45WLP	(0.1060 ± 0.0049)	

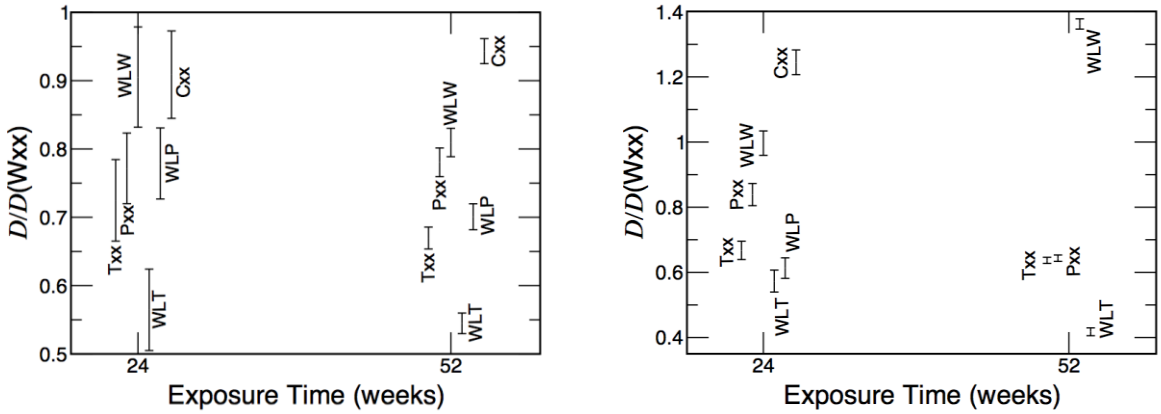

Figure 5. The ratio of the estimated diffusivity D to the diffusivity D(Wxx) estimated for the Wxx sample of the same w/c ratio and exposure time. The results on the left are for the w/c=0.40 mortars, and the results on the right are for the w/c=0.45 mortars.

The performance of any given approach for reducing the diffusion coefficient can be characterized by the ratio of its Dt/R^2 value to the value for that of the ordinary portland cement (OPC) mortar (Wxx). Because the measurements were made at the same time, and because the cylinder radii are constant, these ratios represent the ratio of Fickian diffusivities. These ratios for the w/c=0.40 and the w/c=0.45 are shown separately in Figure 5. In both cases, the WLT

specimens had the lowest relative diffusivities, with the effectiveness increasing over time. For the *w/c*=0.45 mortars, the WLT mortar had a diffusivity that was less than half that of the Wxx mortar after 52 weeks exposure to a chloride solution. Therefore, the expected service life of the WLT mortar, in an environment where diffusion was the controlling transport mechanism, would be twice that of the Wxx mortar.

The effectiveness of saturated LWA, on the whole, seems to depend upon the *w/c* value and the use of a viscosifier. For the *w/c*=0.40 mortars, LWA improved performance, with the addition of a viscosifier also having a positive effect. For the *w/c*=0.45 mortars, however, water-filled LWA (WLW) had higher diffusivities than the Wxx mortar, and the polypropylene-filled LWA (WLP) had an even higher diffusivity; the chloride profile for the WLP specimen was nearly horizontal.

A review of the mass change data in Table 4 above suggests that absorption of the chloride solution by LWA does not provide a convenient explanation for the behavior. The WLT samples had the smallest effective chloride diffusivities, yet also had the second greatest mass increases at both exposure times and both *w/c* values. Although water content plays an important role in providing pathways for diffusion, so does the connectivity of the pore structure. It would appear that the role that the water plays in changing the microstructure of the mortars due to hydration has a greater effect on the diffusivity than merely the total quantity of water.

Thermogravimetric Analysis

Thermogravimetric Analysis (TGA) was applied to investigate the fate of two of the viscosifiers (T and P) within the hydrating cement paste microstructure. Specifically, TGA analysis of the external exposure solution was utilized to examine whether there is significant leaching of the viscosifier from the specimen into the exposure environment, and TGA analysis of broken mortar fragments was utilized to infer the incorporation of the viscosifier into the cement hydration products [19]. Results are provided in Figure 6 and Figure 7. The curves in Figure 6 are the TGA curves for various solutions, indicating that little if any of viscosifier T is present in the 1 yr exposure solution, as the TGA curve for the 1 yr exposure solution is basically identical to that of a freshly prepared 1 mol/L solution of chloride ions, with a peak above 800 °C due to the presence of the chlorides and containing no peaks in the temperature range of 150 °C to 300 °C that would be indicative of the presence of the viscosifier. Similar curves (not shown) were obtained for viscosifier P. Minimal leaching of the viscosifier into the exposure environment is one requirement for the successful long term performance of VERDiCT in field concrete.

Figure 7 indicates that viscosifiers T and P are likely bound, either physically or chemically, within the structure of the cement hydration products, as the two viscosifiers are not volatilized until much higher temperatures in the mortar specimens, compared with the TGA scans for the solutions. The incorporation of polyethylene glycols (somewhat similar in chemical structure to viscosifiers T and P) into the structure of calcium silicate hydrate has been observed by Beaudoin et al. [19]. This would be consistent with the minimal leaching observed for these viscosifiers. The successful performance of these molecules as effective reducers of

diffusivities indicates that such incorporation into the hydration products does not adversely limit their effectiveness in this role.

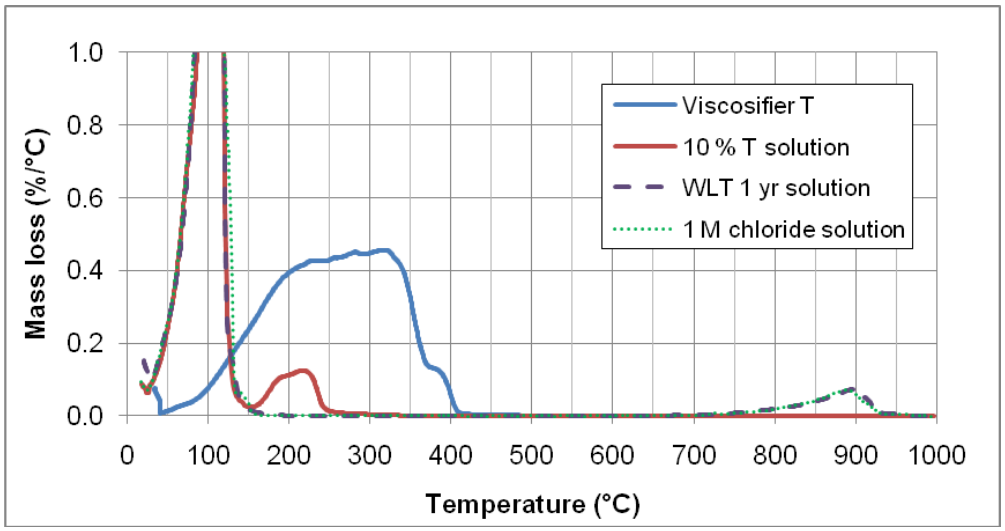

Figure 6. TGA scans for the different solutions as indicated in the legend.

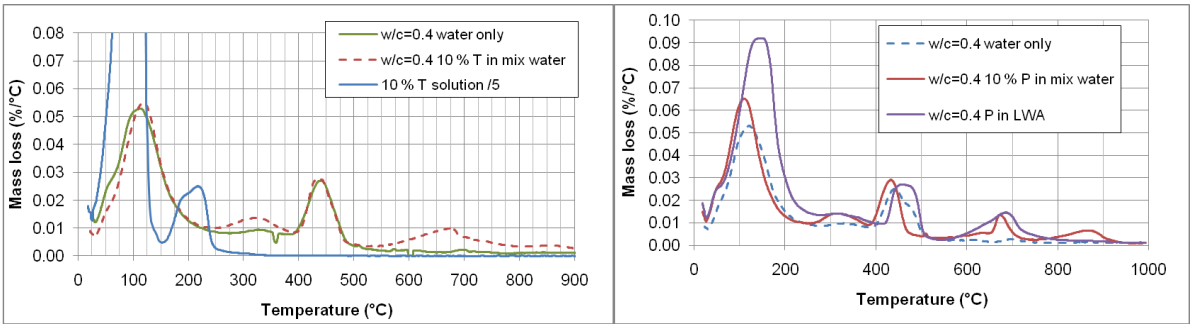

Figure 7. TGA scans for mortar specimens and solutions of viscosifier T (left) and viscosifier P (right). The peak observed above 800 °C for the 10 % P in mix water curve is likely due to the presence of chlorides (see Figure 6 as well).

Conclusions

Ordinary portland cement mortars, having *w/c* mass ratios of 0.40 and 0.45 have been used to demonstrate that the use of viscosity modifiers can successfully reduce the effective diffusivity of chloride ions. After 24 weeks and 52 weeks of submerged exposure to a chloride solution, an analysis of the µXRF profile of chlorine indicates that the effective diffusivity of mortars containing lightweight aggregate saturated with a viscosity modifier can be reduced to approximately one-half the value for a mortar without either LWA or a viscosity modifier. Analysis of the predicted surface concentrations indicates that the measurement technique was consistent over all the samples, and a TGA analysis of the chloride solution and the mortar indicate that the viscosifiers are indeed remaining inside the cement paste.

The approach of using viscosity modifiers to reduce diffusion, demonstrated here in mortars, may provide an alternative method for dramatically increasing the service life of a concrete subjected to diffusion-controlled degradation (e.g., rebar corrosion, sulfate attack, etc.). Further testing on typical concrete formulations is needed to confirm that the viscosifier delivery methods are practical, and that the performance seen thus far is not an artifact of testing on mortars.

Acknowledgements

The authors would like to acknowledge BASF, Lehigh Cement Corporation, Northeast Solite, and SE Tylose for providing materials for the present study. They would also like to thank Drs. William Strawderman and Stefan Leigh of the NIST Statistical Engineering Division for their guidance in formulating the approach used to characterize the uncertainty in the estimated diffusion coefficients, and Mr. Max Peltz of the Engineering Laboratory for his assistance in preparing specimens and conducting the experimental measurements.

References

[1] Lippiatt, B.C., "BEES 4.0 Building for Environmental and Economic Sustainability Technical Manual and User Guide," NISTIR 7423, U.S. Department of Commerce, 2007.
[2] Cusson, D., Lounis, Z., and Daigle, L., "Benefits of Internal Curing on Service Life and Life-Cycle Cost of High-Performance Concrete Bridge Decks – A Case Study," *Cement and Concrete Composites*, **32** (5), 339-350, 2010.
[3] American Concrete Institute, "Report on Early-Age Cracking: Causes, Measurement, and Mitigation," ACI 231R-10, 2010.
[4] Bentz, D.P., Snyder, K.A., Cass, L.C., and Peltz, M.A., "Doubling the Service Life of Concrete. I: Reducing Ion Mobility Using Nanoscale Viscosity Modifiers," *Cement and Concrete Composites*, **30** (8), 674-678, 2008.
[5] Bentz, D.P., Peltz, M.A., Snyder, K.A., and Davis, J.M., "VERDiCT: Viscosity Enhancers Reducing Diffusion in Concrete Technology," *Concrete International*, **31** (1), 31-36, 2009.
[6] Bentz, D.P., Snyder, K.A., and Peltz, M.A., "Doubling the Service Life of Concrete Structures. II: Performance of Nanoscale Viscosity Modifiers in Mortars," *Cement and Concrete Composites*, **32** (3), 187-193, 2010.
[7] Bentz, D.P., "Capitalizing on Self-Desiccation for Autogenous Distribution of Chemical Admixtures in Concrete," in Proceedings of the 4th International Seminar on Self-Desiccation and Its Importance in Concrete Technology, Eds. B. Persson, D. Bentz, and L.-O. Nilsson, Lund University, Lund, 189-196, 2005.
[8] Shimizu, T., and Kenndler, E., "Capillary Electrophoresis of Small Solutes in Linear Polymer Solutions: Relation between Ionic Mobility, Diffusion Coefficient, and Viscosity," *Electrophoresis*, **20**, 3364-3372, 1999.
[9] ASTM C150. Standard Specification for Portland Cement; 2009.
[10] ASTM C185. Standard Test Method for Air Content of Hydraulic Cement Mortar; 2008.
[11] ASTM C305. Standard Practice for Mechanical Mixing of Hydraulic Cement Pastes and Mortars of Plastic Consistency; 2006.

[12] Bentz, D.P., "Influence of Internal Curing Using Lightweight Aggregates on Interfacial Transition Zone Percolation and Chloride Ingress in Mortars," *Cement and Concrete Composites*, **31** (5), 285-289, 2009.
[13] Davis, J.M., Newbury, D.E., Ritchie, N.W.M., Vincenzi, E., Bentz, D., and Fahey, A., "Bridging the Micro to Macro Gap: A New Application for Milli-probe X-ray Fluorescence," accepted by *Microscopy and Microanalysis*, 2010.
[14] Jensen, O.M., Hansen, P.-F., Coats, A.M., and Glasser, F.P., "Chloride Ingress in Cement Paste and Mortar," *Cement and Concrete Research*, **29** (9), 1497-1504, 1999.
[15] Bright, D. (2000). Lispix: Image Processing and Data Visualization Tool for the PC and Macintosh. *Scanning , 22*, 111-112.
[16] Crank, J., *The Mathematics of Diffusion*, Second Edition, Oxford Science Publications, Oxford, 1975.
[17] Abramowitz, M. and Stegun, I.A., *Handbook of Mathematical Functions*, Dover Publications, New York, 1972. (see also http://dlmf.nist.gov)
[18] Taylor, B.N. and Kuyatt, C.E., "Guidelines for Evaluating and Expressing the Uncertainty of NIST Measurement Results," NIST Technical Note 1297, National Institute of Standards and Technology, Department of Commerce, January 1993.
[19] Beaudoin, J. J., Drame, H., Raki, L., and Alizadeh, R., "Formation and Properties of C-S-H-PEG Nanostructures," *Materials and Structures*, **42** (7), 1003-1014, 2008.